Nitric oxide promotes endothelial cell survival signaling through S-nitrosylation and activation of dynamin-2

Ningling Kang-Decker[1,*], Sheng Cao[1,*,‡], Suvro Chatterjee[1], Janet Yao[1], Laurence J. Egan[1], David Semela[1], Debabrata Mukhopadhyay[2] and Vijay Shah[1,‡]

[1]GI Research Unit, Department of Physiology and Tumor Biology Program and [2]Department of Biochemistry and Molecular Biology, Mayo Clinic, Rochester, MN 55903, USA

*These authors contributed equally to this work
‡Authors for correspondence (e-mail: cao.sheng@mayo.edu; shah.vijay@mayo.edu)

Accepted 20 November 2006
Journal of Cell Science 120, 492-501 Published by The Company of Biologists 2007
doi:10.1242/jcs.03361

Summary

Endothelial cell-based angiogenesis requires activation of survival signals that generate resistance to external apoptotic stimuli, such as tumor necrosis factor-alpha (TNF-α), during pathobiologic settings. Mechanisms by which this is achieved are not fully defined. Here, we use a model in which the multifunctional cytokine nitric oxide counterbalances TNF-α-induced apoptosis, to define a role for membrane trafficking in the process of endothelial cell survival signaling. By perturbing dynamin GTPase function, we identify a key role of dynamin for ensuing downstream endothelial cell survival signals and vascular tube formation. Furthermore, nitric oxide is directly demonstrated to promote dynamin function through specific cysteine residue nitrosylation, which promotes endocytosis and endothelial cell survival signaling. Thus, these studies identify a novel role for dynamin as a survival factor in endothelial cells, through a mechanism by which dynamin S-nitrosylation regulates the counterbalances of TNF-α-induced apoptosis and nitric oxide-dependent survival signals, with implications highly relevant to angiogenesis.

Supplementary material available online at
http://jcs.biologists.org/cgi/content/full/120/3/492/DC1

Key words: Endocytosis, Apoptosis, Angiogenesis

Introduction

Tumor necrosis factor-alpha (TNF-α) constitutes a prominent apoptotic stimulus for endothelial cells (EC) in pathobiologic conditions (Zhang et al., 2005). Conversely, nitric oxide (NO) signals are known to mediate cell survival and resistance to apoptosis, a key component of EC-based angiogenesis (Zeng et al., 2001). The mechanisms that regulate this counterbalance of external apoptotic stimuli and survival signaling are not fully defined.

Pathways by which extracellular ligand binding to membrane receptors regulates downstream effectors of EC survival are susceptible to endocytosis-dependent regulation (Bhattacharya et al., 2005; Gliki et al., 2001; Pierce et al., 2000). In this regard, the dynamin family of large GTPase are recognized as drivers of both clathrin and caveolar vesicle internalization (Henley et al., 1998; Oh et al., 1998; Sontag et al., 1994). Thus, the relationship between dynamin and ensuing downstream signal transduction, which regulates the counterbalances of EC survival and apoptosis, may be significant. This is especially true in EC in which the dynamin-2 isoform is closely associated with key EC survival proteins, including the NO generating enzyme, endothelial NO synthase (eNOS), and the VEGF receptor, KDR (Bhattacharya et al., 2005; Chatterjee et al., 2003; Predescu et al., 2001).

Dynamin endocytic function is regulated through post-translational modifications including tyrosine phosphorylation (Ahn et al., 2002; Shajahan et al., 2004). NO also confers post-translational modifications on specific target proteins, especially eNOS binding partners, through S-nitrosylation of specific cysteine residues (Stamler et al., 2001). Since eNOS and dynamin interact closely within cells (Chatterjee et al., 2003; Icking et al., 2005; Wang et al., 2006), in the present study we explored the role of NO regulation of dynamin function as a membrane trafficking switch that regulates EC survival signaling.

Results

Dynamin-dependent endocyotosis promotes EC survival signaling

Endocytic internalization of caveolar receptors and proteins is important for the propagation of several survival signaling pathways (Lua and Low, 2005; Pierce et al., 2000). Since the large GTPase dynamin-2 is essential for endocytosis and downstream signal transduction (Praefcke and McMahon, 2004; Shajahan et al., 2004), and TNF-α is a prototypical apoptotic ligand in EC (Zhang et al., 2005), we examined the effect of dynamin inhibition on TNF-α-induced apoptosis. Transfection of EC with the well-characterized GTPase mutant, K44A, in the form of an adenoviral construct (AdK44A), increased EC apoptosis in response to TNF-α as measured by levels of cleaved caspase-3 from cell lysates (Fig. 1A). As a complementary approach to ascertain the influence of dynamin inhibition on EC survival signaling, we also depleted dynamin from EC using a siRNA approach. Initial

Journal of Cell Science

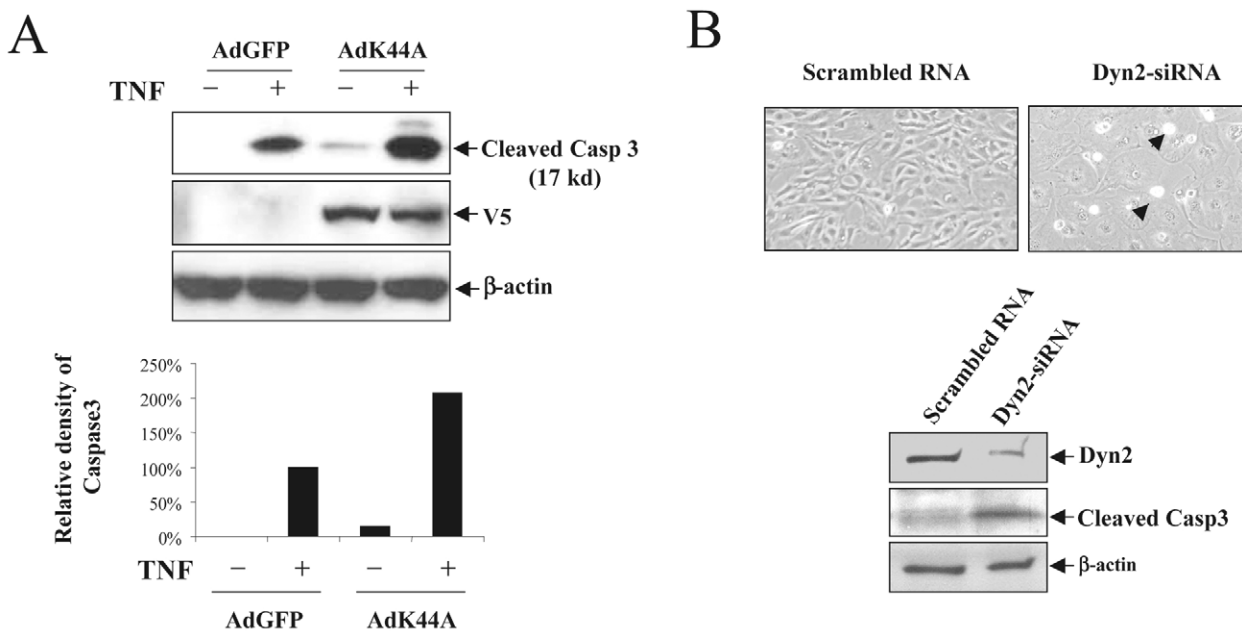

Fig. 1. Inhibition of dynamin GTPase abrogates EC survival signals. (A) BAEC transfected with AdGFP or AdK44A were incubated with vehicle or TNF-α. Cells were collected 24 hours later and prepared for western blot analysis of cleaved caspase-3. Cells transfected with AdK44A showed enhanced TNF-α-induced BAEC apoptosis as demonstrated by a significant increase in the amount of cleaved caspase-3 from cell lysates. Blots were reprobed with V5 antibody or β-actin for verification of the expression of V5-K44A fusion protein and for protein loading control, respectively (*n*=3 separate experiments). (B) EC were transfected with dynamin-2 siRNA or scrambled siRNA and cells were harvested for western blot analysis after 48-72 hours or viewed by microscopy for cell morphology. (Top) Prominent morphologic changes and cell death (arrowheads) were detected in EC transfected with dynamin-2 siRNA. (Bottom) EC transfected with dynamin-2 siRNA showed increased levels of cleaved caspase-3 (*n*=4 separate cell preparations).

experiments evidenced the high transfection efficiency of siRNA in bovine aortic endothelial cells (BAEC) and specificity of the dynamin-2 siRNA (Fig. S1A,B in supplementary material). As shown in Fig. 1B, even in the absence of an apoptotic stimulus, dynamin-2 knockdown from EC resulted in prominent changes in EC morphology and increased EC death as assessed by caspase-3 activation and morphologic detection of apoptotic EC. These data indicate that dynamin promotes survival signaling in EC.

NO promotes EC survival through a dynamin-dependent pathway

NO has been implicated in EC survival signaling through multiple mechanisms (Papapetropoulos et al., 2001; Rossig et al., 2000). Since dynamin and eNOS interact within EC (Chatterjee et al., 2003; Wang et al., 2006), we next explored the hypothesis that NO may reciprocally regulate dynamin function and thereby promote EC survival signals. First, to examine the effects of endogenous eNOS-derived NO on EC survival, we transfected EC with eNOS-siRNA or scrambled RNA and examined activated caspase-3 levels as a measure of apoptosis in the presence of TNF-α and/or the eNOS agonist, VEGF. Initial experiments evidenced the specificity and effectiveness of the eNOS-siRNA to reduce eNOS protein levels and activity in EC (see Fig. S1C in supplementary material). Although VEGF-stimulated NO production protected EC from TNF-α-induced apoptosis, this was not evident in eNOS-siRNA-transfected cells [Fig. 2A; representative western blot with triplicate samples (upper panel), densitometric quantification of pooled experiments (lower panel)]. Transfection of EC with eNOS-siRNA did not result in large levels of caspase-3 cleavage in the absence of an apoptotic stimlus such as TNF-α (data not shown). In a complementary approach, EC were incubated with TNF-α alone or in combination with VEGF and/or the NOS inhibitor L-NAME for 24 hours and analyzed for apoptosis by Hoechst 33342 stain. VEGF reduced TNF-α-induced apoptosis in an L-NAME-inhibitable manner (Fig. S2A in supplementary material). Next, as a complementary approach to assess the effects of NO, we used the NO donor sodium nitroprosside (SNP; 100 μM). SNP protected EC from TNF-α-induced apoptosis as evidenced by diminished levels of TNF-α-induced activated caspase-3 (Fig. 2B; representative western blot with triplicate samples (upper panel) and densitometric analysis (lower panel)]. This protective effect of SNP was observed at concentrations as low as 0.01 μM and was observed in response to an alternative NO donor, S-nitrosoglutathione (GSNO), as well (Fig. S2B in supplementary material). These studies confirm an important role for NO in EC survival signaling.

Next, we directly examined whether NO survival signals could be transduced through dynamin. EC were transfected with AdGFP or AdK44A and then incubated with TNF-α and/or SNP. Although SNP protected EC from TNF-α-induced apoptosis in cells transfected with AdGFP, this protection was not evident in EC transfected with AdK44A [Fig. 3A; representative western blot for cleaved caspase-3 levels (left panel) and densitometric analysis (right panel)]. AdK44A also blocked EC tube formation in response to endogenous NO generated by VEGF (Fig. 3B), demonstrating a physiologic

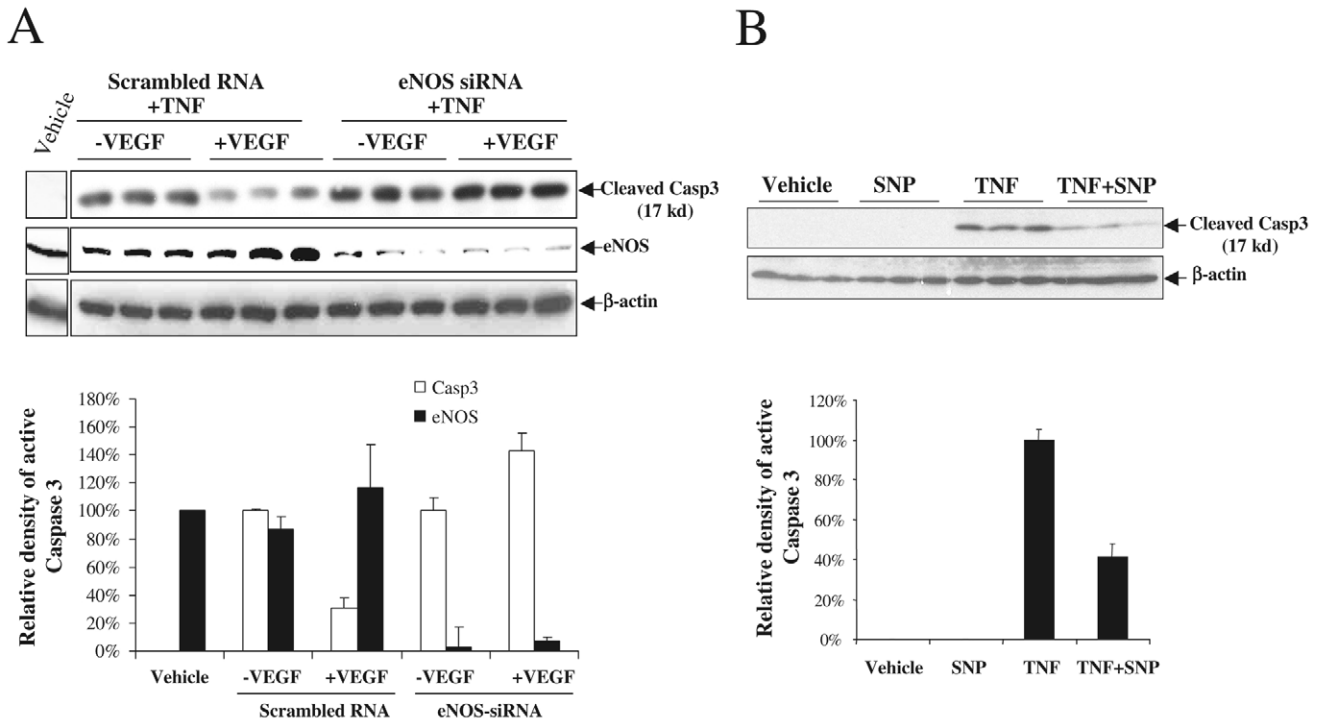

Fig. 2. Endogenous and exogenous NO promotes survival signals that counterbalance TNF-α-induced EC apoptosis. (A) BAEC transfected with scrambled siRNA or eNOS-siRNA were incubated with TNF-α and/or VEGF for 24 hours. Cells were harvested for western blot using antibodies for cleaved caspase-3. VEGF protected cells from TNF-α-induced apoptosis as shown by the reduced level of cleaved caspase-3 from cell lysates. However, VEGF protection was completely abrogated in cells transfected with eNOS-siRNA. The blot was reprobed with β-actin for a control of protein loading, and for eNOS to confirm siRNA knockdown. (B) BAEC were treated with SNP or TNF-α or both and collected for protein extraction and western blot. TNF-α treatment of cells resulted in increased levels of activated caspase-3. Levels of activated caspase-3 were diminished in cells treated with SNP and TNF-α when compared with cells treated with TNF-α alone. A representative panel of western blots of triplicate experiments is shown in the top panel, with densitometric analysis of pooled experiments shown in the bottom panel.

relevance of dynamin-dependent EC survival signals in the context of angiogenesis.

To examine whether dynamin-dependent NO survival signaling occurs through the prototypical downstream cGMP-protein kinase G (PKG) pathway, cells were pretreated with equimolar concentrations of SNP (100 μM) or the cGMP analogue and PKG agonist 8-Br-cGMP, prior to incubation with TNF-α. Although SNP protected EC from TNF-α-induced apoptosis, no protection was afforded by 8-Br-cGMP even up to a concentration of 100 μM and in the presence of adenoviral overexpression of Flag-tagged PKG (AdPKG; Fig. 3C). As a positive control, 8-Br-cGMP did increase EC migration at this concentration, as previously noted by others (Kawasaki et al., 2003) (vehicle: 100% and 8-Br-cGMP: 283%; *n*=3), and the PKG construct increased PKG activity from cell lysates of transfected cells by 2.5-fold (relative activity/mg protein; AdGFP: 27.7 versus AdPKG: 69.3). Thus, NO, independent of the prototypical cGMP-PKG pathway, counterbalances TNF-α-induced apoptosis in EC in a dynamin-dependent manner.

NO activates dynamin GTPase activity through S-nitrosylation

Since inhibition of dynamin GTPase activity prevented NO-dependent EC survival signaling, we next directly examined whether NO promotes dynamin-dependent endocytosis. EC were preincubated with the NO donor GSNO (100 μM) or vehicle for 10 minutes and assayed for uptake of fluorescence-conjugated transferrin (Tfn), a marker of clathrin-dependent endocytosis, or lactosylceramide (LacCer), a marker of caveolae-dependent endocytosis (Henley et al., 1998; Oh et al., 1998). Fluorescent ligand uptake was analyzed quantitatively using a highly sensitive laser scanning cytometry (LSC) method and also measured qualitatively by confocal microscopy. Incubation of EC with GSNO increased Tfn (Fig. 4A) and LacCer (Fig. 4B) uptake as compared with vehicle (Tfn: control R1=6%, GSNO R1=15%. LacCer: control R1=13%, GSNO R1=55%). To directly test whether these effects of NO were mediated through activation of dynamin GTPase, EC were transfected with mock virus or AdK44A prior to GSNO incubation as the mutant lacks GTPase domain function, rendering it resistant to GTPase domain activation. AdK44A blocked Tfn uptake as previously noted (Altschuler et al., 1998) and more importantly, GSNO did not increase Tfn uptake in EC transfected with AdK44A (control R1=27%, K44A R1=17%, K44A+GSNO R1=18%) (Fig. 4C). These data demonstrate that NO promotes dynamin GTPase activity and endocytosis.

Dynamin endocytic function is regulated in part by its GTPase activity (Altschuler et al., 1998). To directly assess

Journal of Cell Science

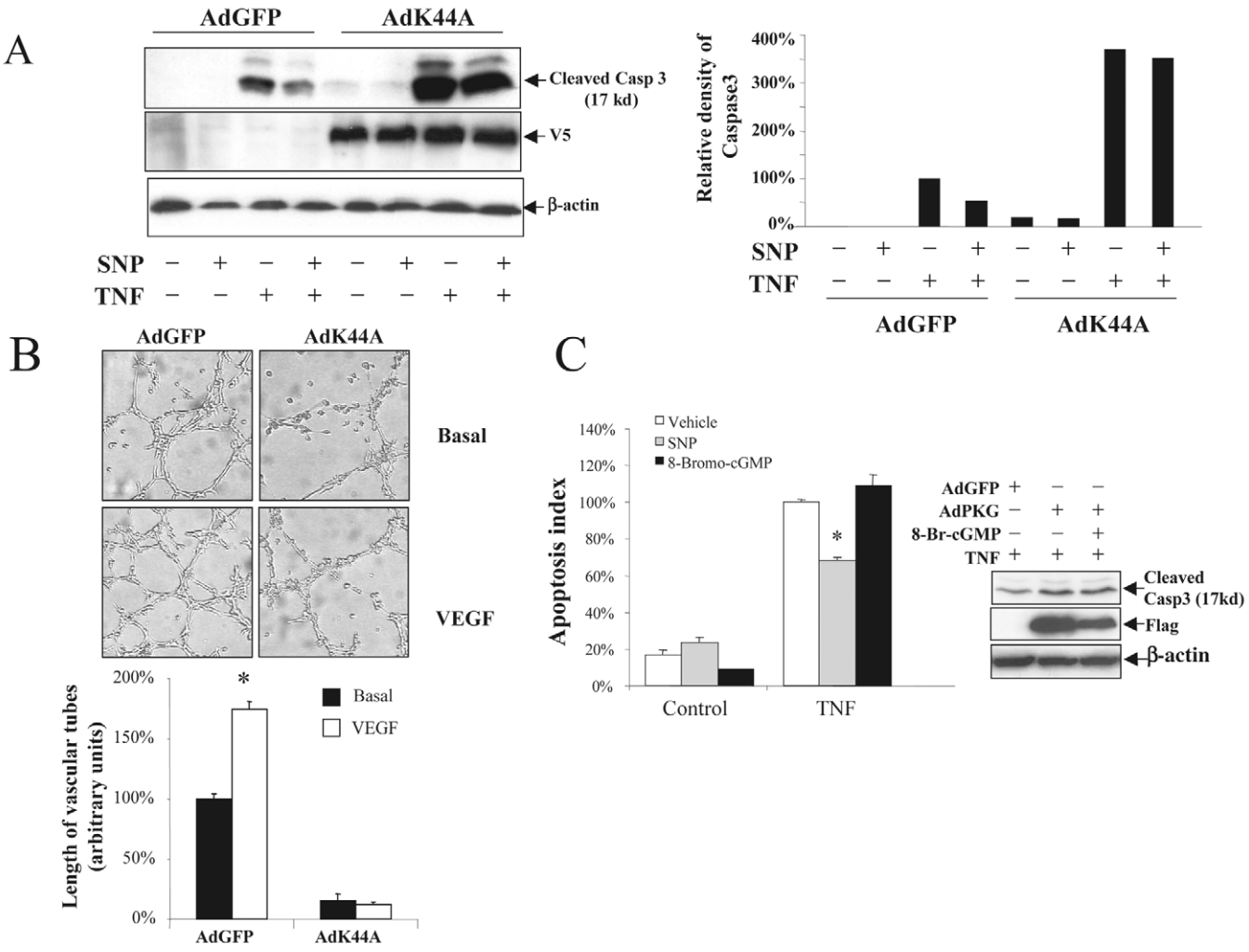

Fig. 3. NO survival signals are independent of the cGMP-PKG pathway and require dynamin. (A) BAEC transfected with AdGFP or AdK44A were incubated with SNP or TNF-α or both. Cells were collected 24 hours later and prepared for western blot analysis of cleaved caspase-3. Cells transfected with AdK44A showed enhanced TNF-α-induced BAEC apoptosis as demonstrated by a significant increase in the amount of cleaved caspase-3 from cell lysates. In the presence of K44A overexpression, SNP-dependent protection from TNF-α-induced apoptosis was attenuated [representative blot (left panel) and densitometric analysis (right panel); n=5]. Blots were reprobed with anti-V5 antibody or anti β-actin antibody for verification of the expression of V5-K44A fusion protein and for protein loading control, respectively. (B) Tube formation in response to VEGF was assessed by the tube formation assay on Matrigel in EC transfected with AdGFP or AdK44A. Twenty-four hours after transduction, 30,000 cells were seeded in Matrigel-coated wells and the length of endothelial tubes after 12 hours was measured. In GFP-transfected EC, VEGF significantly promoted tube formation (*P<0.05 versus respective basal medium). By contrast, K44A-transfected BAEC failed to form tubes (n=3). Representative phase-contrast images of experimental conditions are shown in the upper panels and compiled data are shown in the graph (lower panel). (C) Left, BAEC were treated with TNF-α and co-incubated with SNP, 8-Br-cGMP or vehicle for 24 hours. Apoptosis was assessed by Hoechst 33342 stain, and TNF-induced apoptosis was assigned a relative value of 100%. SNP reduced TNF-α-induced apoptosis whereas 8-Br-cGMP did not (*P<0.05; TNF-α+SNP versus TNF-α alone; n=3). Right, BAEC were transfected with adenoviruses encoding GFP (AdGFP) or flag-tagged wild-type PKG (AdPKG), and treated with TNF-α alone or in combination with 8-Br-cGMP. Cell lysates were prepared 24 hours later for western blot analysis. Neither overexpression of PKG nor combination of PKG with the agonist 8-Br-cGMP protected cells from TNF-α-induced apoptosis. PKG expression was verified by the presence of Flag epitope.

whether NO activates dynamin GTPase function, we pursued in vitro GTPase activity studies to measure the catalytic activity of purified recombinant dynamin in the presence and absence of GSNO. A representative experiment is shown in Fig. 4D, demonstrating that GSNO increases dynamin GTPase activity by 300% compared with dynamin alone (lane 4 versus lane 3). Similar results were obtained with an alternative NO donor, diethylamine NONOate (DEA-NO) (data not shown). These studies indicate that NO donors can enhance dynamin GTPase activity and promote endocytosis.

As NO-based nitrosylation influences vesicle exocytosis (Matsushita et al., 2003) and NO can act independently of the canonical cGMP-PKG survival pathway in EC, we next considered whether NO promotes dynamin function through nitrosylation. Indeed, while these studies were near completion, a paper was published demonstrating that the dynamin-1 isoform of the dynamin GTPase family is a target

Journal of Cell Science

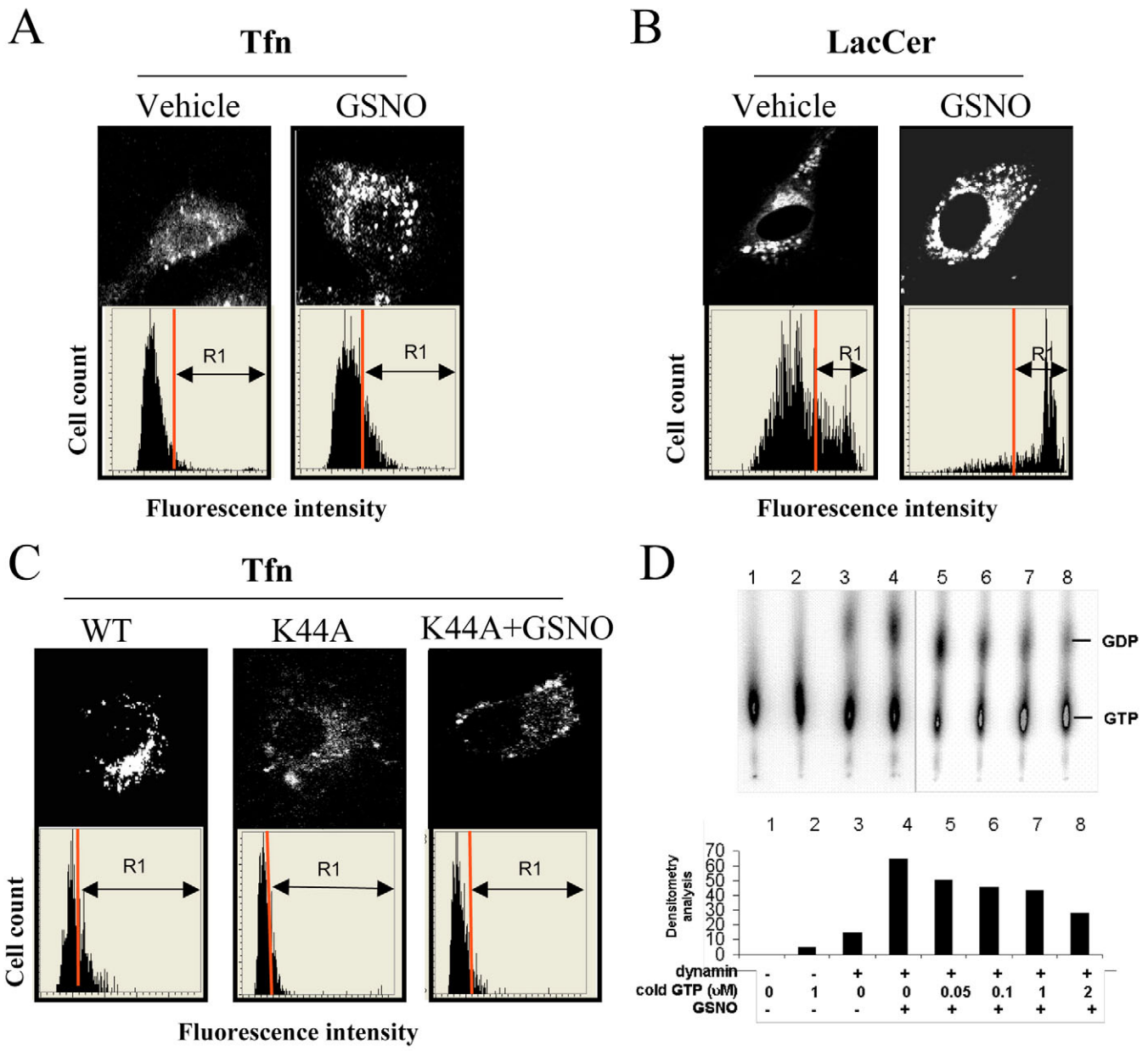

Fig. 4. NO donors increase endocytosis by augmenting dynamin GTPase activity. (A,B) BAEC were preincubated with vehicle or the NO donor GSNO for 20 minutes and then further incubated with fluorescent ligands [fluorescent 488 conjugated transferrin (Tfn) or BODIPY C5-lactosylceramide (LacCer)] for 10 minutes and analyzed by laser scanning cytometry and confocal fluorescence microscopy. Tfn uptake was increased in cells incubated with GSNO as compared with vehicle. Upper panels show representative cell captured by confocal microscopy and lower panels show quantitation by laser scanning cytometry (control R1=6%, GSNO R1=15%). LacCer uptake was also increased in cells incubated with GSNO (control R1=13%, GSNO R1=55%). (C) BAEC were transfected with wild-type dynamin virus or AdK44A prior to GSNO, and Tfn uptake was assayed. AdK44A transduction of EC reduced Tfn uptake and blocked NO-induced increase of Tfn uptake (left: control R1=27%; middle: K44A R1=17%; right: K44A+GSNO R1=18%). (D) Dynamin GTPase activity was measured by thin-layer chromatographic detection of GDP from GTP using recombinant GST-dynamin and a representative experiment is shown. Dynamin incubated with GSNO resulted in an increase in GDP and depletion of GTP, indicating activation of GTPase activity (lane 4). Increased cold GTP competes the conversion from ^{32}P-labeled GTP to GDP (lanes 5-8). Densitometric analysis of the experiment is shown in the lower panel. This experiment was repeated three times with similar results.

for nitrosylation by NO in a process that promotes internalization of pathogens into cells (Wang et al., 2006). To directly examine whether dynamin-2 is a nitrosylation target of NO, we used the biotin-switch method and UV-visible spectroscopy (Jaffrey et al., 2001). Nitrosylation of immunoprecipitated EC dynamin was detected in response to GSNO (100 μM), whereas nitrosylation was not detected in the absence of GSNO (Fig. 5A, left). The NO donor, DEA-NO (100 μM), also nitrosylated purified recombinant GST-dynamin as well as its GTPase domain (Fig. 5A, right). By

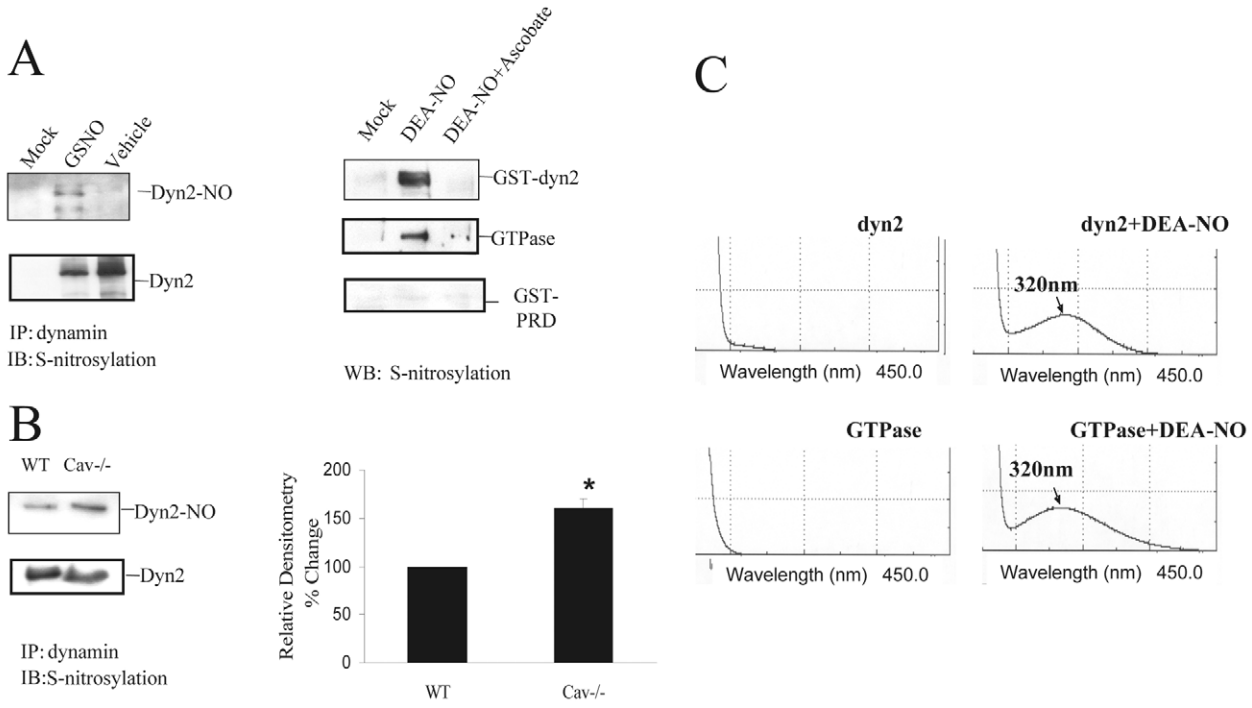

Fig. 5. NO nitrosylates dynamin. (A) Purified recombinant GST-dynamin, specific subdomains or immunoprecipitated dynamin from cells were incubated with GSNO or vehicle. Alternatively, dynamin was immunoprecipitated from aortic lysates of caveolin wild-type or caveolin-null mice. Nitrosylation of dynamin-2 was assessed by biotin-switch method. S-nitrosylation of immunoprecipitated dynamin from cells is shown (left) [anti-biotin (top panel) and anti-dyn2 (bottom panel)]. Mock represents immunoprecipitation with non-immune serum. Full-length GST dynamin, as well as the GTPase subdomain, showed nitrosylation by DEA-NO. Nitrosylation signal was blocked by preincubation of cells with the reducing agent, ascorbic acid. GST-PRD-domain nitrosylation was not detected. (B) Dynamin nitrosylation was also increased in dynamin-2 immunoprecipitates prepared from aortic lysates of mice genetically deficient in caveolin as compared with wild-type samples (left panel shows a representative autoradiograph and the right panel shows the quantitative change from three independent pooled experiments; $*P<0.05$). (C) Purified GST-dynamin or the GTPase subdomain were incubated with the NO donor, DEA-NO, or vehicle and then prepared for spectrophotometric analysis. GST-dynamin and the GST-GTPase domain alone incubated with vehicle show a flat curve throughout 200 nm to 450 nm; however, after incubation with GSNO, a characteristic S-nitrosylation peak was detected at ~320 nm.

contrast, biotin switch did not reveal prominent nitrosylation of the GST-PRD domain (see GST-PRD, bottom-right in Fig. 5A), providing evidence that GST nitrosylation was not confounding the biotin-switch assay. Dynamin nitrosylation was also increased in aortic tissues of mice genetically deficient in caveolin-1, which show a phenotype of increased basal NO generation (Razani et al., 2002), supporting the concept of NO-dependent dynamin nitrosylation in situ (Fig. 5B). Although cells from these mice are devoid of caveolae (Razani et al., 2002), prior work has demonstrated that caveolar proteins such as eNOS and dynamin may reside in non-caveolar compartments such as Golgi and lipid rafts (Cao et al., 2001; Shah et al., 1997; Sowa et al., 2001). Thus, dynamin may be exposed to eNOS-derived NO gradients within one of these subcellular compartments in $Cav^{-/-}$ EC. We confirmed dynamin nitrosylation by UV-visible spectrophotometric analysis, an alternative method to detect nitrosothiol modification of proteins (Jaffrey et al., 2001). As seen in Fig. 5C, incubation of dynamin or the GTPase subdomain with DEA-NO revealed an absorbance peak at ~320 nm, reflecting the light absorbance changes indicative of a nitrosothiol bond. However, the recombinant protein alone, in the absence of incubation with a NO donor, did not reveal an absorbance peak at 320 nm. Furthermore, no absorbance peak was detected with the NO donor alone, in the absence of recombinant protein (data not shown).

Finally, to directly demonstrate that NO survival signals could indeed promote EC survival through a dynamin-dependent pathway, we next sought to identify the specific cysteine residue that was responsible for the functional effects observed in response to dynamin nitrosylation. There are two cysteine residues in the dynamin-2 GTPase domain. We pursued a site-directed mutagenesis strategy in which each of these cysteines (C24 and C86) was changed to an alanine, a residue that is not susceptible to nitrosylation. Constructs were subcloned into a retroviral expression vector to allow for high-level overexpression in BAEC. Since NO promoted endocytosis in EC through a dynamin-dependent pathway, we first examined NO-induced endocytosis in BAEC transfected with the various mutant constructs. As seen in Fig. 6A, BAEC transfected with C86A had no significant increase in endocytosis in response to GSNO (control R1=10%, GSNO R1=12%). Conversely, NO-induced endocytosis was maintained in BAEC transfected with C24A (control R1=12%, GSNO R1=65%). We also examined the effects of the mutants in our model of TNF-α-induced apoptosis. Overexpression of C86A, but not C24A, abolished the protection conferred by NO donors in the face of TNF-α-induced apoptosis (Fig. 6B). A

Journal of Cell Science

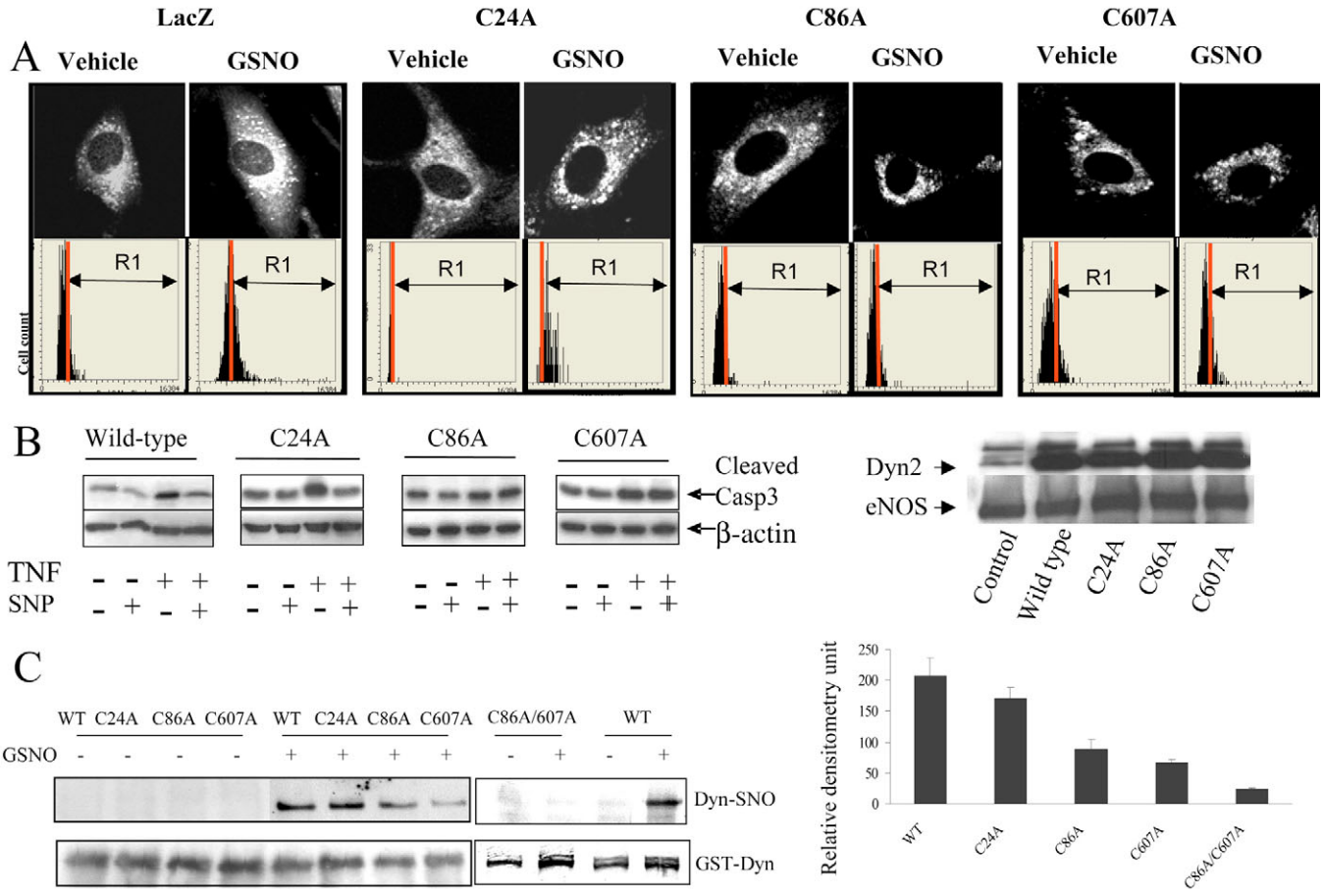

Fig. 6. Nitrosylation of cysteine 86 and cysteine 607 of dynamin-2 regulates NO activation of dynamin and survival signals. BAEC were transfected with retroviral vectors encoding LacZ, wild-type dynamin-2 or mutant dynamin constructs, C24A, C86A or C607A. (A) Cells were preincubated with vehicle or the NO donor (GSNO, 20 minutes) and then LacCer uptake was measured using laser scanning cytometry and confocal fluorescence microscopy. LacCer uptake was increased in cells transfected with LacZ that were incubated with GSNO as compared with vehicle (control R1=7%, GSNO R1=18%). The second panel shows cells transfected with C24A, which also shows increased uptake of LacCer in response to GSNO (control R1=12%, GSNO R1=65%). The remaining two panels show cells transfected with C86A or C607A, which show no significant increase of endocytosis in response to GSNO (control R1=10%, GSNO R1=12% and control R1=11%, GSNO R1=12%, respectively). Upper panels show representative cells captured by confocal microscopy and lower panels show quantitation of histograms by laser scanning cytometry (n=3 independent experimental preparations). (B) Transfected cells were incubated with SNP or TNF-α or both and collected 24 hours later and prepared for western blot analysis of cleaved caspase-3. Although SNP conferred protection against TNF-α-induced apoptosis in BAEC that express C24A mutant, overexpression of either C86A or C607A abolished SNP-induced protection from TNF-α-induced apoptosis. Apoptosis was assessed by measuring levels of cleaved caspase-3 from cell lysates. The blots were probed with anti-β-actin antibody to confirm equal protein loading. The far-right panel western blot shows similar levels of overexpressed dynamin lysates from each of the experimental groups and the increase in dynamin protein levels compared with non-transfected control cell lysates. (C) Purified recombinant GST-dynamin-2 or single-/double-point mutant proteins were incubated with GSNO or vehicle and nitrosylation was assessed by biotin-switch method. Nitrosylation in response to GSNO was detected with the wild-type dynamin protein. An attenuated nitrosylation signal was detected with the C86A and C607A single-point mutant proteins, whereas GSNO-induced nitrosylation was almost undetectable in the C86/C607A double-mutant protein. Quantitative analysis of the level of nitrosylation of the mutant constructs in response to GSNO is shown in the graph to the right.

recent publication that emanated during the conduct of our studies revealed that nitrosylation of dynamin-1 at amino acid 607 in the PH domain regulated microbe internalization (Wang et al., 2006). Since this cysteine residue at amino acid 607 is conserved in dynamin-2, we mutated this residue to alanine as well to examine its effect on NO survival signaling. Interestingly, the C607A construct showed a phenotype similar to the C86A construct. For example, cells transfected with C607A showed neither GSNO-induced endocytosis (Fig. 6A; R1=11%, GSNO R1=12%) nor SNP-induced protection from TNF-α-induced apoptosis (Fig. 6B). To confirm that C86 and C607 of dynamin-2 could indeed both be nitrosylated by NO, we performed biotin-switch assays using purified recombinant protein constructs. Although dynamin nitrosylation was detected in both the C86A and C607A mutant proteins, nitrosylation was not detected in a mutant protein in which both C86 and C607 were changed to alanine (Fig. 6C). In summary, these studies indicate that both C86 and C607 are

Journal of Cell Science

Journal of Cell Science

crucial for NO-mediated protection against TNF-α-induced apoptosis.

Discussion

EC-based angiogenesis and vascular homeostasis are governed by a counterbalance of opposing EC survival signals and apoptosis signals. In this regard, the present studies provide novel observations that enhance our understanding of this process. We find that inhibition of dynamin GTPase function markedly perturbs EC survival signaling and that activation of dynamin promotes EC survival signals. Notably, we identify a mechanism by which NO activates dynamin through post-translational S-nitrosylation. Thus, these studies delineate a novel cross-talk between TNF-α-driven apoptosis signals and NO survival signaling that is regulated by dynamin nitrosylation, thereby uncovering a surprising and novel angiogenic capacity for dynamin GTPase in EC.

The role of NO in EC survival is controversial as NO promotes EC survival through numerous potential mechanisms but may also promote apoptosis through a mitochondrial pathway (Rossig et al., 2000). Adding to this complexity is the diversity in signaling pathways by which NO effects on EC survival are conferred (Kawasaki et al., 2003; Rossig et al., 2000). In the present study, NO survival signals did not transduce through the canonical cGMP-PKG pathway, and thus prompted us to examine alternative mechanisms of NO signaling. Increasing evidence indicates a key role for S-nitrosylation of NO target proteins, whereby NO reacts with specific cysteine thiols to form an S-nitrosylated derivative that regulates the biological activity of the target protein (Iwakiri et al., 2006; Stamler et al., 2001; Williams et al., 2003). Thus, NO signaling in EC appears to occur through complementary cGMP-dependent and -independent pathways. Indeed, in neuronal cells, recent studies have delineated a complex interplay of both cGMP-dependent and nitrosylation-dependent pathways by which NO promotes neuronal survival, thereby providing interesting parallels with NO signaling in EC (Ciani et al., 2002; Riccio et al., 2006). Interestingly, Ras GTPase, one of the most established nitrosylation targets of NO, demonstrates GTPase activation in response to nitrosylation, and maintains a GTPase domain architecture that is comparable to the dynamin GTPase domain (Williams et al., 2003). This prompted us to query and then establish, through the use of several complementary approaches, that dynamin-2 is indeed a NO nitrosylation target that can promote NO-dependent EC survival.

Since NO increased dynamin GTPase activity and endocytosis, we anticipated that cysteine nitrosylation may occur in the GTPase subdomain. Indeed, sequence analysis of the GTPase domain of dynamin-2 revealed two cysteines within the GTPase domain: C24 and C86. Although mutation of C24 did not influence NO activation of endocytosis and survival signaling, mutation of C86 prevented NO-dependent endocytosis and survival signaling. In fact, amino acids 85-87 of dynamin-2 (His85-Cys86-Lys87) constitutes a putative 'nitrosylation motif' whereby a hydrophobic cysteine is juxtaposed with hydrophilic residues (histine and lysine). Extrapolation of this sequence to the crystal structure of the GTPase domain of dynamin (Protein Data Bank ID code 2AKA) (Reubold et al., 2005) reveals that this cysteine is exposed to the surface of the molecule, in close apposition to the GTP-binding pocket, and also within a proximity of 6 Å to aromatic amino acids (phenylalanines 83 and 91). This proximity to aromatic amino acids has been postulated to enhance cysteine-nitrosylation susceptibility based on computer modeling studies (Hao et al., 2006). Interestingly, in the course of our work, a paper was published by Wang et al. that demonstrated that NO nitrosylates the dynamin-1 isoform of the dynamin GTPase family (Wang et al., 2006). In that study, nitrosylation was demonstrated to occur at cysteine 607 within the PH domain of dynamin-1. Since this cysteine is conserved within the dynamin-2 isoform as well, we examined this residue as a possible NO nitrosylation target in dynamin-2. Similar to that observed with the C86 mutant, the C607 mutant also prevented NO endocytosis and survival signaling in EC. Thus, the current studies corroborate the recent work by Wang et al. (Wang et al., 2006) and mechanistically extend that work, by demonstrating an essential role for nitrosylation of both C86 and C607 of dynamin-2. These studies also extend the work of Wang et al. by demonstrating an important role for dynamin nitrosylation in the process of EC survival signaling and angiogenesis.

The present studies are of particular interest in relation to the role of dynamin in the prototypical VEGF pathway of signaling in EC (Papapetropoulos et al., 2001). Prior studies from our group and others have demonstrated that perturbation of dynamin function alters the localization and function of both eNOS and the VEGF receptor, KDR, with ensuing impairment of VEGF signaling and eNOS activation (Bhattacharya et al., 2005; Cao et al., 2001; Maniatis et al., 2006). The present studies extend these concepts by demonstrating that inhibition of dynamin function in EC potentiates EC apoptosis and antagonizes EC survival signaling. Interestingly, in epithelial-type cells which, unlike EC, do not utilize a VEGF-NO survival pathway, dynamin overexpression has been shown to inhibit cell survival signals (Fish et al., 2000), indicating a cell-type specificity of dynamin membrane trafficking functions.

Thus, the present studies highlight a novel mechanism by which NO survival signaling in EC is conferred. Furthermore, they identify dynamin, through its regulation of membrane traffic, as an EC-specific survival factor that regulates the coordinated balances of apoptosis, survival and ensuing EC-based angiogenesis.

Materials and Methods

Cell culture and transfection

BAEC (P2-6; Clonetics, San Diego, CA) were used in these studies. Cells were cultured in Dulbecco's modified Eagle's medium (DMEM) supplemented with 10% fetal bovine serum (FBS), penicillin (100 IU/ml) and streptomycin (100 IU/ml). Pharmacologic reagents used in these studies included L-NAME (1 mM), 8-Br-cGMP (100 μM), VEGF-165 (10 ng/ml for migration and 50 ng/ml for survival studies) and TNF-α (30 ng/ml). Complementary NO donor compounds were used for various assays described below, at doses that did not exceed 100 μM, a concentration threshold commonly used for in vitro studies (Nisoli et al., 2005). Transfection of BAEC was performed with siRNA, adenoviral vectors or retroviral vectors. siRNA transfection was performed using Oligofectamine reagent (Invitrogen) with a final concentration of 100 nM. Functional and biochemical assays were performed between 48 and 72 hours after transfection. Replication-incompetent serotype 5 adenoviral vectors included a well-characterized GTPase domain point mutant, K44A, that functions as a dominant negative for GTP-dependent dynamin functions (Chatterjee et al., 2003) (AdK44A; University of Iowa Vector Core), wild-type PKG (AdPKG; K. Bloch, Massachusetts General Hospital, Boston, MA) and green fluorescent protein (GFP) (AdGFP; Bill Sessa, Yale University). For adenoviral transduction, BAEC were transfected with PBS/0.1% albumin containing 50 MOI (multiplicity of infection) of adenovirus for 1 hour. The

Journal of Cell Science

vector solution was then aspirated and, after washing with PBS, complete culture medium was replenished. Transfection efficiency using this approach was at almost 100%. The retroviruses were produced from a 293T packaging cell line (Zeng et al., 2002). In brief, 293T cells were grown to 30-40% confluency and cotransfected with pMD.MLV gag.pol, pMD.G and pMMP vectors containing the cDNA sequence of interest. Cell culture supernatant containing high-titer viruses were collected after 48 hours. For transduction of EC, cells were grown to 40-50% confluency and retroviral stock was added to the culture medium at a ratio of 1:4 with polybrene 4-8 μg/ml. Cells were utilized for functional and biochemical assays after 24 hours.

Plasmid and retrovirus construction

Dynamin-2 constructs (provided courtesy of Mark McNiven, Mayo Clinic, Rochester, MN) were subcloned into the GST fusion protein vector pGEX-1. GST constructs were transformed into BL21 (DE3) and purified as we described previously (Cao et al., 2001). Specificity and quality of GST-dynamin-2 constructs were assessed by Coomassie Blue staining. Point mutations of cysteine 24, 86 and 607 to alanine were generated by PCR (QuikChange; Stratagene) using three pairs of primers; 5′-CGGTCAGAGCGCCCACCTGGACC-3′, 5′-GTTTTTGCACGCC-AAGTCCAAAA-3′ and 5′-CGAACTGGCTGCCGACTCCCAGG-3′, respectively. Constructs were subcloned into the pMMP retroviral vector or pGEX-1 GST vectors using standard molecular biology approaches. All constructs were verified by sequencing.

Expression and purification of recombinant proteins

Recombinant dynamin protein and subdomains were purified from *Escherichia coli* as previously described (Cao et al., 2001). In brief, dynamin, its subdomains or mutants in the GST plasmid were transformed into BL21 (DE3), induced with isopropyl β-D-thiogalactopyranosid (IPTG) (1 mM) overnight, and lysed by sonication with lysozyme. Samples were resonicated after addition of Triton X-100 to a final concentration of 1%. Cell debris was removed by centrifugation and supernatant was mixed with glutathione sepharose beads and agitated for 2 hours at 4°C. Samples were centrifugated and pellets washed three times in PBS with 1% Triton X-100. Specificity and quality of GST fusion proteins was assessed by Coomassie Blue staining of SDS-PAGE gels.

Dynamin GTPase activation assay

Dynamin (0.5 μM) was incubated with or without the NO donor GSNO (100 μM) for 30-60 minutes at room temperature in a buffer (135 mM NaCl, 5 mM KCl, 20 mM HEPES, pH 7.4, 1 mM MgCl2) as previously described (Ahn et al., 2002). Reactions (20 μl) were initiated by the addition of 10 μCi/ml [α-^{32}P] GTP. GTP hydrolysis was analyzed by thin-layer chromatography on PEI cellulose (Sigma), and results were quantified using phosphorImager and ImageQuant software (Molecular Dynamics, Sunnyvale, CA). Quantitation of cold GTP and GDP at each time point was performed on a PhosphorImager (Molecular Dynamics).

UV-visible spectrophotometric analysis

Recombinant proteins were incubated with or without the NO donor DEA NONOate (DEA-NO; 50 μM) for 20-60 minutes and passed through a Sephadex G-60 column to remove the NO donor. The S-nitrosylation characteristic absorbance peak at 320-340 was measured by 200-450 nm UV-visible wavelength scanning (Jaffrey et al., 2001).

Biotin-switch method

Recombinant proteins were diluted or mouse aorta/treated cells were lysed in HEN buffer [250 mM HEPES, pH 7.7, 1 mM EDTA, 0.1 mM neocuproine, 1% Nonidet P-40, 150 mM NaCl, 1 mM PMSF, protease inhibitor mixture (Sigma)] as we and others have previously done (Jaffrey et al., 2001; Perri et al., 2006). GSNO (100 μM) or DEA-NO (50 μM) was added to the protein solution or cell lysates for 20 minutes in the dark. The solution or lysates were then mixed with an equal volume of methyl methanethiosulfonate (MMTS) buffer (25 mM HEPES, pH 7.7, 0.1 mM EDTA, 10 μM neocuproine, 5% SDS, 20 mM MMTS) and incubated at 50°C for 20 minutes with frequent vortexing. After free MMTS was removed by acetone precipitation, the precipitates were resuspended in HENS buffer (25 mM HEPES, pH 7.7, 0.1 mM EDTA, 10 μM neocuproine, 1% SDS). After adding 50 mM ascorbate in the mixture, to reduce non-modified SNO, the S-nitrosylated proteins were then modified with biotin in HPDP buffer (25 mM HEPES, pH 7.7, 0.1 mM EDTA, 1% SDS, 10 μM neocuproine, 10 mM ascorbic acid sodium salt and 0.2 mM N-[6-(biotinamido)hexyl]-3′-(2′-pyridyldithio) propionamide (biotin-HPDP; Pierce). Mixture was vortexed and allowed to react at room temperature for 1 hour in the dark. The samples were then added to Laemmli buffer without a reducing reagent and separated by SDS-PAGE followed by immunoblotting with anti-biotin antibody (Cell Signaling). In some experiments, cells were subjected to NO donor and, after cell lysates were immunoprecipitated with anti-dynamin antibody (Transduction Laboratories), the immunoprecipitates were blocked with MMTS and subsequent modification with biotin-HPDP. In some experiments, to establish specificity of nitrosylation, cells were incubated with ascorbic acid (2.5 mM) in conjunction with the NO donor.

Endothelial tube formation assay

Tube formation assays were performed as we have previously described (Gulati et al., 2003). In brief, four slide chambers (Lab-Tek Chamber Slides, Nunc) were coated with 150 μl Matrigel per chamber (10 ng/ml, BD Biosciences) and incubated at 37°C for 30 minutes to promote gelling. Twenty-four hours after transduction with AdGFP or AdK44A, BAEC [1×10^5 cells in 1000 μl of DMEM medium containing 1% of basal endothelial growth supplement (ECGS, ScienCell)] were seeded in each of the Matrigel-coated wells. VEGF or vehicle was added to the Matrigel-coated wells and, after 12 hours of incubation at 37°C in a 5% CO_2 humidified atmosphere, the center of each well was photographed (three consecutive pictures) with a light microscope. The length of the tubes was measured at 100× magnification with Image-Pro Plus (Media Cybernetics, version 5.1). All assays were done in three independent experiments.

Western blot

After transfection with the appropriate adenovirus and/or siRNA and incubation with test compounds, BAEC were collected and lysed in a buffer (50 mM Tris, 01 mM EDTA, 0.1 mM EGTA, 0.1%SDS, 1% NP-40, 0.1% deoxycholic acid, pH 7.5) (Cao et al., 2001). Lysates were prepared for measurement of caspase-3 after 24 hours of incubation with test compounds. Protein lysates were prepared and quantified using Bio-Rad protein assay. Equal amounts of protein (30 μg/well) were loaded and separated by SDS-PAGE and transferred to PVDF membranes. After blocking, blots were incubated with primary antibody (GAPDH mAb, Ambion; eNOS mAb, Transduction Laboratories; caspase-3 Ab, Cell Signaling; β-actin Ab, Sigma; Flag M2 Ab, Sigma; dynamin pAb, Transduction Laboratories) for 2 hours at room temperature or overnight at 4°C, incubated with appropriate secondary antibody, and protein-band signals detected with ECL (Amersham Biosciences). Quantification was performed by densitometric analysis of band density using the software ImageJ (NIH).

Confocal fluorescence microscopy

For imaging of fluorescent-labeled molecule uptake, cells were preincubated with the NO donor GSNO (100 μM) or vehicle for 10 minutes and then incubated with 5 μg/ml Tfn Alexa-Fluor 488 or 0.5-2.5 μM BODIPY C5-lactosylceramide (LacCer). After a series of washing steps to remove residual fluorescent lipid remaining at the plasma membrane, cells were fixed with 1% paraformaldehyde, stained with Hoechst and mounted for analysis. For apoptosis detection, 0.3×10^6 BAEC were seeded into each well of six-well plates. Cells were transfected with appropriate adenovirus or siRNA and/or treated with test compounds at concentrations as indicated. Floating cells together with the remaining attached cells were collected and fixed with 4% formaldehyde. Cell pellets were suspended in Hoechst 33342 (10 μg/ml) and apoptotic cells were identified by conventional fluorescence microscopy (5100TV; Zeiss, Germany) based on the presence of chromatin condensation and nuclear fragmentation. Each experimental condition was examined for apoptosis in triplicate with 1000 cells from four different high-power fields. Each experiment was performed on three independent occasions.

Imaging cytometer analysis

Quantification of endocytosis was performed using an inverted-format laser scanning cytometer (LSC; iCyte-Compucyte, Cambridge, MA). This system has a large field of depth, so cells are illuminated uniformly throughout their volume, which allows accurate whole-cell immunofluorescence intensity measurements with objective and quantitative analysis (Dmitrieva et al., 2004). Fluorescent-labeled Tfn uptake and BODIPY-LacCer internalization were measured to assess clathrin- and caveolae-mediated endocytosis, respectively (Henley et al., 1998; Oh et al., 1998). In brief, after incubation of cells with NO donor and fluorescent compounds as described above, two to three areas (5×5 mm^2) were chosen in each chamber for fluorescence intensity measurement. Cells were recognized by LSC by nuclear Hoechst stain and cytoplasmic green fluorescence was counted per cell and plotted as a histogram as previously described (Ozawa et al., 2005). Green fluorescence intensity cut lines were calculated between the groups to quantitatively analyze endocytosis of the fluorescent compounds. Histograms were quantitated as the percentage of cells with fluorescent intensity above the specified cut-point (R1), with the same cutpoint applied to all samples within a given experiment.

Statistical analysis

Statistical analyses were performed using Student's *t*-test. $P<0.05$ was considered as statistically significant.

The authors thank Martin Fernando-Zapico and Raul Urrutia for critical review of the manuscript, Mark McNiven for providing dynamin subdomain constructs and Resham Bhattacharya and Yehia Daaka for helpful discussions. These studies were supported by R01 DK59615, R01 DK59388 and P50CA102701 Pancreatic Cancer SPORE Development Grant (V.S.) and an American Heart Association Scientist Development Grant (AHA0435063N to S.C.).

Journal of Cell Science

References

Ahn, S., Kim, J., Lucaveche, C. L., Reedy, M. C., Luttrell, L. M., Lefkowitz, R. J. and Daaka, Y. (2002). Src-dependent tyrosine phosphorylation regulates dynamin self-assembly and ligand-induced endocytosis of the epidermal growth factor receptor. *J. Biol. Chem.* **277**, 26642-26651.

Altschuler, Y., Barbas, S. M., Terlecky, L. J., Tang, K., Hardy, S., Mostov, K. E. and Schmid, S. L. (1998). Redundant and distinct functions for dynamin-1 and dynamin-2 isoforms. *J. Cell Biol.* **143**, 1871-1881.

Bhattacharya, R., Decker, N., Hughes, D., Priyabrata, M., Shah, V., McNiven, M. and Mukhopadhyay, D. (2005). Regulatory role of dynamin-2 in VEGFR-2/KDR-mediated endothelial signaling. *FASEB J.* **19**, 1692-1694.

Cao, S., Yao, Y., McCabe, T., Yao, Q., Katusic, Z., Sessa, W. and Shah, V. (2001). Direct interaction between endothelial nitric-oxide synthase and dynamin-2. Implications for nitric-oxide synthase function. *J. Biol. Chem.* **276**, 14249-14256.

Chatterjee, S., Cao, S., Petersen, T., Simari, R. and Shah, V. (2003). Inhibition of GTP-dependent vesicle trafficking impairs internalization of plasmalemmal eNOS and cellular nitric oxide production. *J. Cell Sci.* **116**, 3645-3655.

Ciani, E., Guidi, S., Bartesaghi, R. and Contestabile, A. (2002). Nitric oxide regulates cGMP-dependent cAMP-responsive element binding protein phosphorylation and Bcl-2 expression in cerebellar neurons: implication for a survival role of nitric oxide. *J. Neurochem.* **82**, 1282-1289.

Dmitrieva, N. I., Cai, Q. and Burg, M. B. (2004). Cells adapted to high NaCl have many DNA breaks and impaired DNA repair both in cell culture and in vivo. *Proc. Natl. Acad. Sci. USA* **101**, 2317-2322.

Fish, K., Schmid, S. and Damke, H. (2000). Evidence that dynamin-2 functions as a signal-transducing GTPase. *J. Cell Biol.* **150**, 145-154.

Gliki, G., Abu-Ghazaleh, R., Jezequel, S., Wheeler-Jones, C. and Zachary, I. (2001). Vascular endothelial growth factor-induced prostacyclin production is mediated by a protein kinase C (PKC)-dependent activation of extracellular signal-regulated protein kinases 1 and 2 involving PKC-delta and by mobilization of intracellular Ca2+. *Biochem. J.* **353**, 503-512.

Gulati, R., Jevremovic, D., Peterson, T. E., Chatterjee, S., Shah, V., Vile, R. G. and Simari, R. D. (2003). Diverse origin and function of cells with endothelial phenotype obtained from adult human blood. *Circ. Res.* **93**, 1023-1025.

Hao, G., Derakhshan, B., Shi, L., Campagne, F. and Gross, S. S. (2006). SNOSID, a proteomic method for identification of cysteine S-nitrosylation sites in complex protein mixtures. *Proc. Natl. Acad. Sci. USA* **103**, 1012-1017.

Henley, J., Krueger, E., Oswald, B. and McNiven, M. (1998). Dynamin-mediated internalization of caveolae. *J. Cell Biol.* **141**, 85-99.

Icking, A., Matt, S., Opitz, N., Wiesenthal, A., Muller-Esterl, W. and Schilling, K. (2005). NOSTRIN functions as a homotrimeric adaptor protein facilitating internalization of eNOS. *J. Cell Sci.* **118**, 5059-5069.

Iwakiri, Y. S. A., Chatterjee, S., Shah, V., Chalouni, C., Toomre, D., Fulton, D., Groszmann, R. J. and Sessa, W. C. (2006). Nitric oxide synthase establishes a local nitric oxide gradient regulating S-nitrosylation and protein secretion. *Proc. Natl. Acad. Sci. USA* **103**, 19777-19782.

Jaffrey, S., Erdjument-Bromage, H., Ferris, C., Tempst, P. and Snyder, S. (2001). Protein s-nitrosylation: a physiological signal for neuronal nitric oxide. *Nat. Cell* **3**, 193-197.

Kawasaki, K., Smith, R. J., Hsieh, C., Sun, J., Chao, J. and Liao, J. (2003). Activation of the phosphatidylinositol 3-kinase/protein kinase Akt pathway mediates nitric oxide-induced endothelial cell migration and angiogenesis. *Mol. Biol. Cell* **23**, 5726-5737.

Lua, B. L. and Low, B. C. (2005). Activation of EGF receptor endocytosis and ERK1/2 signaling by BPGAP1 requires direct interaction with EEN/endophilin II and a functional RhoGAP domain. *J. Cell Sci.* **118**, 2707-2721.

Maniatis, N. A., Brovkovych, V., Allen, S. E., John, T. A., Shajahan, A. N., Tiruppathi, C., Vogel, S. M., Skidgel, R. A., Malik, A. B. and Minshall, R. D. (2006). Novel mechanism of endothelial nitric oxide synthase activation mediated by caveolae internalization in endothelial cells. *Circ. Res.* **99**, 870-877.

Matsushita, K., Morrell, C., Cambien, B., Yang, S., Yamakuchi, M., Bao, C., Hara, M., Quick, R. and Lowenstein, C. (2003). NO regulates exocytosis by S-nitrosylation of NSF. *Cell* **115**, 139-150.

Nisoli, E., Tonello, C., Cardile, A., Cozzi, V., Bracale, R., Tedesco, L., Falcone, S., Valerio, A., Cantoni, O., Clementi, E. et al. (2005). Calorie restriction promotes mitochondrial biogenesis by inducing the expression of eNOS. *Science* **310**, 314-317.

Oh, P., McIntosh, P. and Schnitzer, J. E. (1998). Dynamin at the neck of caveolae mediates their budding to form transport vesicles by GTP-driven fission from the plasma membrane of endothelium. *J. Cell Biol.* **141**, 101-114.

Ozawa, K., Hudson, C. C., Wille, K. R., Karaki, S. and Oakley, R. H. (2005). Development and validation of algorithms for measuring G-protein coupled receptor activation in cells using the LSC-based imaging cytometer platform. *Cytometry A* **65**, 69-76.

Papapetropoulos, A., Garcia-Cardena, G., Madri, J. and Sessa, W. (2001). Nitric oxide production contributes to the angiogenic properties of vascular endothelial growth factor in human endothelial cells. *J. Clin. Invest.* **100**, 3131-3139.

Perri, R. E., Langer, D. A., Chatterjee, S., Gibbons, S. J., Gadgil, J., Cao, S., Farrugia, G. and Shah, V. H. (2006). Defects in cGMP-PKG pathway contribute to impaired NO dependent responses in hepatic stellate cells upon activation. *Am. J. Physiol. Gastrointest. Liver Physiol.* **290**, G535-G542.

Pierce, K. L., Maudsley, S., Daaka, Y., Luttrell, L. M. and Lefkowitz, R. J. (2000). Role of endocytosis in the activation of the extracellular signal-regulated kinase cascade by sequestering and nonsequestering G protein-coupled receptors. *Proc. Natl. Acad. Sci. USA* **97**, 1489-1494.

Praefcke, G. J. and McMahon, H. T. (2004). The dynamin superfamily: universal membrane tubulation and fission molecules? *Nat. Rev. Mol. Cell Biol.* **5**, 133-147.

Predescu, S. A., Predescu, D. N. and Palade, G. E. (2001). Endothelial transcytotic machinery involves supramolecular protein-lipid complexes. *Mol. Biol. Cell* **12**, 1019-1033.

Razani, B., Combs, T. P., Wang, X. B., Frank, P. G., Park, D. S., Russell, R. G., Li, M., Tang, B., Jelicks, L. A., Scherer, P. E. et al. (2002). Caveolin-1-deficient mice are lean, resistant to diet-induced obesity, and show hypertriglyceridemia with adipocyte abnormalities. *J. Biol. Chem.* **277**, 8635-8647.

Reubold, T. F., Eschenburg, S., Becker, A., Leonard, M., Schmid, S. L., Vallee, R. B., Kull, F. J. and Manstein, D. J. (2005). Crystal structure of the GTPase domain of rat dynamin 1. *Proc. Natl. Acad. Sci. USA* **102**, 13093-13098.

Riccio, A., Alvania, R. S., Lonze, B. E., Ramanan, N., Kim, T., Huang, Y., Dawson, T. M., Snyder, S. H. and Ginty, D. D. (2006). A nitric oxide signaling pathway controls CREB-mediated gene expression in neurons. *Mol. Cell* **21**, 283-294.

Rossig, L., Haendeler, J., Hermann, C., Malchow, P., Urbich, C., Zeiher, A. and Dimmeler, S. (2000). Nitric oxide down-regulates MKP-3 mRNA levels: involvement in endothelial cell protection from apoptosis. *J. Biol. Chem.* **275**, 25502-25507.

Shah, V., Haddad, F., Garcia-Cardena, G., Frangos, J., Mennone, A., Groszmann, R. and Sessa, W. (1997). Liver sinusoidal endothelial cells are responsible for nitric oxide modulation of hepatic resistance. *J. Clin. Invest.* **100**, 2923-2930.

Shajahan, A. N., Timblin, B. K., Sandoval, R., Tiruppathi, C., Malik, A. B. and Minshall, R. D. (2004). Role of Src-induced dynamin-2 phosphorylation in caveolae-mediated endocytosis in endothelial cells. *J. Biol. Chem.* **279**, 20392-20400.

Sontag, J. M., Fykse, E. M., Ushkaryov, Y., Liu, J. P., Robinson, P. J. and Sudhof, T. C. (1994). Differential expression and regulation of multiple dynamins. *J. Biol. Chem.* **269**, 4547-4554.

Sowa, G., Pypaert, M. and Sessa, W. (2001). Distinction between signaling mechanisms in lipid rafts vs. caveolae. *Proc. Natl. Acad. Sci. USA* **98**, 14072-14077.

Stamler, J., Lamas, S. and Fang, F. (2001). Nitrosylation: the prototypic redox-based signaling mechanism. *Cell* **106**, 675-683.

Wang, G., Moniri, N. H., Ozawa, K., Stamler, J. S. and Daaka, Y. (2006). Nitric oxide regulates endocytosis by S-nitrosylation of dynamin. *Proc. Natl. Acad. Sci. USA* **103**, 1295-1300.

Williams, J. G., Pappu, K. and Campbell, S. L. (2003). Structural and biochemical studies of p21Ras S-nitrosylation and nitric oxide-mediated guanine nucleotide exchange. *Proc. Natl. Acad. Sci. USA* **100**, 6376-6381.

Zeng, H., Sanyal, S. and Mukhopadhyay, D. (2001). Tyrosine residues 951 and 1059 of vascular endothelial growth factor receptor-2 (KDR) are essential for vascular permeability factor/vascular endothelial growth factor-induced endothelium migration and proliferation, respectively. *J. Biol. Chem.* **276**, 32714-32719.

Zeng, H., Zhao, D. and Mukhopadhyay, D. (2002). KDR stimulates endothelial cell migration through heterotrimeric G protein Gq/11-mediated activation of a small GTPase RhoA. *J. Biol. Chem.* **277**, 46791-46798.

Zhang, W., Zheng, S., Storz, P. and Min, W. (2005). Protein kinase D specifically mediates apoptosis signal-regulating kinase 1-JNK signaling induced by H2O2 but not tumor necrosis factor. *J. Biol. Chem.* **280**, 19036-19044.